# *Streptococcus pneumoniae* Isoprenoid Biosynthesis Is Downregulated by Diphosphomevalonate: An Antimicrobial Target†

John L. Andreassi, II, Kristina Dabovic, and Thomas S. Leyh*

*Department of Biochemistry, Albert Einstein College of Medicine, 1300 Morris Park Avenue, Bronx, New York 10461-1926*

*Received September 7, 2004; Revised Manuscript Received October 1, 2004*

ABSTRACT: The toll that *Streptococcus pneumoniae* exacts on the welfare of humanity is enormous. This organism claims the lives of ∼3700 people daily, the majority of whom are children below the age of 5, and the situation could worsen due to the increasing incidence of pernicious, multiple-antibiotic-resistant strains. Here we report the discovery and characterization of a new allosteric site, shown to be absent in humans, that can be used to switch off an essential pathway in *S. pneumoniae*, the mevalonate pathway. Diphosphomevalonate (DPM), an intermediate in the pathway, binds with high affinity ($K_d$ = 530 nM) to mevalonate kinase, the first enzyme in the pathway, and inactivates it. Steady-state and equilibrium binding measurements reveal that DPM binding is noncompetitive versus substrates. DPM binds at an allosteric site, and inhibition cannot be overcome by an increasing substrate concentration. The DPM-binding site is a promising target for the development of new antimicrobial agents.

The isoprenoid family consists of roughly 23 000 biologically active, low-molecular mass compounds (*1*). Isoprenoids are found in the membranes of cells; electron transport chains make extensive use of isoprenoid-based redox carriers, the tethers that localize proteins within the cell are synthesized from isoprenoids, as are many heme R-group modifications, steroid hormones, bile acids, carotenoids, and numerous other interesting classes of compounds (*2*, *3*). Given the metabolic importance and ubiquity of these compounds, it is not surprising that a properly functioning isoprenoid biosynthetic pathway is essential for the viability of *Strepococcus pneumoniae* (*4*).

Organisms that utilize the mevalonate pathway synthesize isoprenoids from a single, five-carbon building block, isopentenyl diphosphate, the end product of the mevalonate pathway. The first two steps of the pathway are catalyzed by mevalonate and phosphomevalonate kinase (Figure 1), whose consecutive actions produce diphosphomevalonate (DPM), which is shown below to potently inhibit mevalonate kinase. DPM is then decarboxylated, in an ATP-dependent fashion, to produce isopentenyl diphosphate.

Multiple-drug-resistant strains of *S. pneumoniae* are rapidly proliferating (*5*, *6*). This organism acquires resistance by spontaneous mutagenesis and DNA transfer from related species, and spreads via colonization. Pneumococci inhabit the nasopharynx of ∼15% of well adults and ∼65% of school children (*7*). While many streptococci are managed well with existing antibiotics, certain variants are capable of evading our last-line antibiotics, including vancomycin (*8*−*10*). New targets are critical for sustaining the development of antibiotics needed to maintain control of this deadly organism (*11*). The mevalonate kinase allosteric site, described and characterized here, is one such target.

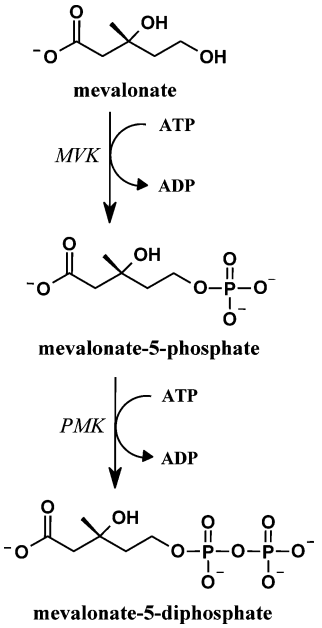


FIGURE 1: Mevalonate pathway. Isopentenyl diphosphate, the end product of the pathway, is the five-carbon unit used in isoprenoid biosynthesis.

## MATERIALS AND METHODS

Lactate dehydrogenase (rabbit muscle) and pyruvate kinase (rabbit muscle) were purchased from Roche Applied Science. Adenosine 5′-($\beta$,$\gamma$-imido)triphosphate (AMP-PNP), ATP, phosphoenolpyruvate (PEP), $\beta$-mercaptoethanol (2-ME),[1] dithiothreitol (DTT), reduced glutathione (GSH), $MgCl_2$, KOH, and $KH_2PO_4$ were purchased from Sigma. NaCl, KCl, Hepes, Tris, glycerol, and Luria-Bertani Miller (LB) medium

† Supported by the National Institutes of Health Grant GM54469 and the Albert Einstein College of Medicine.

* To whom correspondence should be addressed: Department of Biochemistry, Albert Einstein College of Medicine, 1300 Morris Park Ave., Bronx, NY 10461-1926. Phone: (718) 430-2857. Fax: (718) 430-8565. E-mail: leyh@aecom.yu.edu.

10.1021/bi048075t CCC: $27.50 
Published on Web 12/04/2004

were purchased from Fisher Scientific. Isopropyl 1-thio-β-D-galactopyranoside (IPTG) was purchased from Labscientific. Chelating Sepharose Fast Flow and glutathione−Sepharose Fast Flow resins, a Superdex 200 10/300 GL column, and molecular mass standards were acquired from Amersham Biosciences. Competent *Escherichia coli* BL21-(DE3) cells were purchased from Novagen. *S. pneumoniae* (R6) phosphomevalonate kinase was purified using a dual-affinity tag (*12*). Restriction enzymes were purchased from New England Biolabs. (*R*,*S*)-Mevalonate, (*R*)-5-phosphomevalonate, and (*R*)-5-diphosphomevalonate were prepared as described previously (*13*). All other reagents were of the highest commercial grade.

*Expression and Purification of S. pneumoniae MVK*. Recombinant MVK was expressed in BL21(DE3) cells as an amino-terminal GST fusion protein. Cells containing the expression plasmid were grown at 37 °C to an $OD_{600}$ of ∼0.8, and the cultures were then cooled to 17 °C, induced by addition of IPTG (0.70 mM), and incubated at 17 °C for 17 h. The cells were then pelleted, resuspended, lysed by sonication, and prepared for subsequent chromatography as described previously (*13*). The extract was loaded onto a glutathione−Sepharose column, and nontagged contaminants were removed by washing with $KPO_4$ (50 mM), DTT (2.0 mM), and KCl (0.40 M) (pH 7.3). MVK was then eluted using buffer containing Tris (100 mM, pH 8.0), DTT (2.0 mM), GSH (10 mM), and KCl (0.40 M). The GST tag was removed from the MVK fusion using Prescission protease during overnight dialysis against Hepes/$K^+$ (25 mM, pH 7.5), KCl (50 mM), and DTT (2.0 mM) at 4 ± 2 °C. The GST tag and protease were then separated from MVK by passing the dialysate over a glutathione−Sepharose resin. The MVK was ∼95% pure, as judged by SDS−PAGE, and stored in 30% glycerol at −70 °C. The protein was quantitated optically at 280 nm ($\epsilon_{280}^* = 22.9\ mM^{-1}\ cm^{-1}$).

*Human MVK*. The full-length human MVK cDNA was purchased from Invitrogen. The MVK coding region was amplified by PCR using gene-specific primers containing an NdeI and XhoI restriction site (underlined) in the forward and reverse primers, respectively (forward, 5′-GGAATTC-CATATGATGTTGTCAGAAGTCCTACTGGTGTCTGC-TCCGG-3′; reverse, 5′-CCGCCGCTCGAGTCAGAGGC-CATCCAGGGCTTGCTGGACTCG-3′). The PCR product was restricted, using NdeI and XhoI, and ligated into the multiple cloning site of a pGEX-6P vector modified to contain a nine-His−GST dual-affinity tag (*12*).

*Expression and Purification of Human Mevalonate Kinase*. Human MVK was expressed in BL21(DE3) cells as described above. The cell extract was loaded onto a $Ni^{2+}$-chelating Sepharose column; contaminants were removed, and MVK was then eluted with imidazole directly onto a glutathione−Sepharose affinity column. Glutathione affinity chromatography and removal of the His−GST tag were performed as described in ref *12*. The purity of the enzyme, as judged by SDS−PAGE, was >95%.

*Initial Rate Measurements*. Initial rates were measured under the 16 conditions defined by a 4 × 4 matrix of reactant concentrations, either two substrates or a substrate and an inhibitor (*13*). Typically, substrate concentrations ranged from $\sim 0.2K_m$ to $5K_m$, and inhibitor concentrations ranged from 0 to $\sim 3K_i$. The concentration of the nonvaried substrate in inhibition experiments was fixed near saturation. Velocities were measured during the first 10% of reaction.

*AMP-PNP versus ATP*. The assay conditions used in the AMP-PNP inhibition studies were as follows: *S. pneumoniae* MVK (30 nM), AMP-PNP (0, 1.1, 2.25, and 3.5 mM), MgATP (0.5, 0.65, 0.9, and 1.5 mM), mevalonate (135 μM, $5K_m$), Hepes/$K^+$ (50 mM, pH 8.0), KCl (50 mM), $MgCl_2$ ([nucleotide] + 1 mM), 2-ME (0.14%), PEP (3.0 mM), NADH (0.28 mM), pyruvate kinase (50 units/mL), and lactate dehydrogenase (20 units/mL), $T = 25$ °C. The concentration of PK was selected to prevent complications caused by AMP-PNP inhibition of PK (*13*). The data were fit to a linear competitive inhibition model using COMP (*14*).

*Initial Rate Constants for the Human Mevalonate Kinase*. $K_{m\ ATP}$ for human MVK was determined at a fixed, near-saturating concentration of mevalonate (250 μM, $7.5K_m$); the ATP concentration was varied from $0.2K_m$ to $30K_m$. The assay conditions were as follows: MVK (0.14 μM), PMK (1.6 units), Hepes/$K^+$ (50 mM, pH 8.0), KCl (50 mM), PK (5.0 units), LDH (10 units), PEP (1.0 mM), 2-ME (0.14%), NADH (0.30 mM), $MgCl_2$ ([nucleotide] + 1.0 mM), and mevalonate (250 μM), $T = 25 \pm 2$ °C. Phosphomevalonate kinase was added to prevent the slight product inhibition caused by phosphomevalonate ($K_{i\ app\ PMev} = 100$ μM, data not shown).

The $K_{m\ Mev}$ for human MVK was determined using a progress curve method in which both products, phosphomevalonate and ADP, are removed by coupling enzymes (*12*). The mevalonate concentration can be calculated at each point in the progress curve from the absorbance changes associated with the oxidation of NADH, which was measured at 339 nm ($\epsilon_{339}^* = 0.0124\ \mu M^{-1}\ cm^{-1}$). The velocity can be determined at each mevalonate concentration by taking a slope of the progress curve at each concentration. The *V* versus [S] data obtained from the curve were fit to the Michaelis−Menten equation. The assay conditions were as follows: human MVK (85 nM), mevalonate (250 μM), ATP (2.0 mM, $30K_m$), $MgCl_2$ ([nucleotide] + 1.0 mM), PMK (1.6 units), Hepes/$K^+$ (50 mM, pH 8.0), KCl (50 mM), PK (5.0 units), LDH (10 units), PEP (1.0 mM), 2-ME (0.14%), and NADH (0.3 mM), $T = 25 \pm 2.0$ °C.

*Native Molecular Mass of S. pneumoniae MVK*. The native molecular mass of MVK was determined by size-exclusion chromatography using a Superdex 200 10/300 GL column calibrated with the following molecular mass standards: ferritin (440 kDa), catalase (232 kDa), albumin (67.0 kDa), ovalbumin (43.0 kDa) and chymotrypsinogen A (25.0 kDa). Chromatography was performed at 25 ± 2 °C using, as the equilibration and running buffer, Hepes/$K^+$ (pH 8.0, 50 mM) and KCl (50 mM). The mass of MVK was calculated from the linear log(mass) versus elution volume plot obtained using the protein standards.

## RESULTS AND DISCUSSION

*Allosteric Downregulation of the Mevalonate Pathway in S. pneumoniae*. The addition of mevalonate to a solution containing mevalonate kinase, ATP, and the pyruvate kinase/

[1] Abbreviations: 2-ME, β-mercaptoethanol; DTT, dithiothreitol; Hepes, *N*-(2-hydroxyethyl)piperazine-*N*′-2-ethanesulfonic acid; Tris, tris(hydroxymethyl)aminomethane; unit, 1 μmol of product formed per minute at a saturating concentration of a substrate(s).

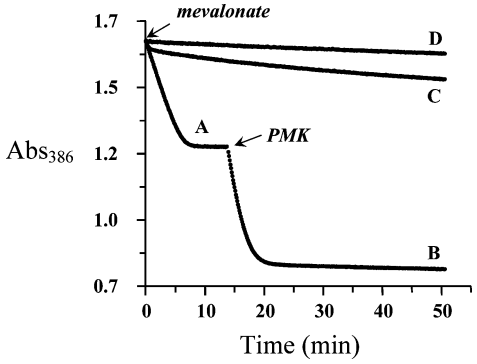


FIGURE 2: Allosteric downregulation of isoprenoid biosynthesis in *S. pneumoniae*. (A) Mevalonate is added (0.70 mM, final) to a reaction mixture containing mevalonate kinase (1.2 $\mu$M), ATP (1.0 mM), and an ATP regenerating system (PK/LDH, see below) that couples the optically detected reduction of $NAD^+$ to product formation. Mevalonate is quantitatively (≥98%) converted to phosphomevalonate. (B) Phosphomevalonate kinase is added to the mixture for reaction A at 14.0 min, resulting in quantitative conversion of phosphomevalonate to diphosphomevalonate. (C) Conditions are identical to those associated with reaction A except that phosphomevalonate kinase (90 nM) is present at time zero. (D) Conditions are identical to those associated with reaction A except that DPM (100 $\mu$M) was present at time zero. All of the reaction mixtures contained pyruvate kinase (10 units/mL), lactate dehydrogenase (20 units/mL), ATP (2.0 mM), $MgCl_2$ (3.0 mM), NADH (2.9 mM, $\epsilon^*_{386} = 0.61\ mM^{-1}\ cm^{-1}$), PEP (4.0 mM), KCl (50 mM), 2-$\beta$ME (0.14%), and Hepes/$K^+$ (50 mM, pH 8.0) at 25 °C.

Table 1: Initial Rate Parameters for the *S. pneumoniae* and Human MVKs

| organism | $K_{i-Mev}$ ($\mu$M) | $K_{m-Mev}$ ($\mu$M) | $K_{i-ATP}$ ($\mu$M) | $K_{m-ATP}$ ($\mu$M) | $k_{cat}$ ($s^{-1}$) |
|---|---|---|---|---|---|
| *S. pneumoniae* | $44 \pm 9.0$[a] | $27 \pm 3.5$ | $1361 \pm 290$ | $844 \pm 109$ | $228 \pm 10$ |
| *Homo sapiens* | ND[b] | $33 \pm 0.1$ | ND | $57 \pm 4.0$ | $20 \pm 0.03$ |

[a] Kinetic constants are shown with their standard errors. [b] Not determined.

lactate dehydrogenase coupling system (which regenerates ATP) results in the quantitative conversion of mevalonate to phosphomevalonate; the subsequent addition of phosphomevalonate kinase quantitatively converts phosphomevalonate to diphosphomevalonate (Figure 2). If, however, both mevalonate and phosphomevalonate kinase are present when mevalonate is added, the reaction velocity decreases relatively quickly, and little product is formed (Figure 2). An important difference between these experiments is that DPM forms *during* net-forward synthesis of phosphomevalonate only if both enzymes are present when mevalonate is added, which suggests that DPM might inhibit mevalonate kinase. This hypothesis was confirmed by demonstrating that mevalonate kinase turnover is inhibited potently by DPM at 100 $\mu$M (Figure 2).

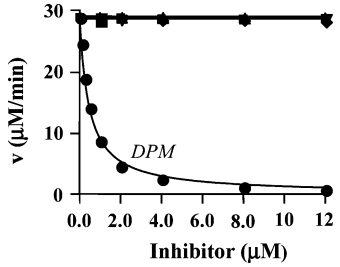


FIGURE 3: *S. pneumoniae* mevalonate kinase inhibition is specific for diphosphomevalonate. The initial rate of the forward reaction of *S. pneumoniae* mevalonate kinase is plotted as a function of the concentration of DPM (●), and each of the four metabolites that lie immediately downstream of DPM in the isoprenoid biosynthetic pathway: isopentenyl diphosphate (◆), dimethylallyl diphosphate (▼), geranyl diphosphate (▲), and farnesyl diphosphate (■). The assay conditions were as follows: mevalonate kinase (48 nM), mevalonate (30 $\mu$M, 1$K_m$), ATP (800 $\mu$M, 1$K_m$), $MgCl_2$ ([nucleotide] + 1 mM), pyruvate kinase (10 units/mL), lactate dehydrogenase (20 units/mL), PEP (3.0 mM), NADH (0.28 mM), KCl (50 mM), 2-$\beta$ME (0.14%), and Hepes/$K^+$ (50 mM, pH 8.0) at 25 ± 2 °C.

*MK Inhibition Is DPM-Specific*. Given their considerable structural similarity to DPM, the four isoprenoid metabolites that lie immediately downstream of DPM (isopentenyl diphosphate, dimethylallyl diphosphate, geranyl diphosphate, and farnesyl diphosphate) were tested as inhibitors of MVK. The effects of titrating DPM and these four metabolites on the initial rate of the forward MK reaction are compared in Figure 3. Turnover of the enzyme is inhibited at low concentrations of DPM ($IC_{50} = 0.45\ \mu M$) and virtually unaffected by the other metabolites at concentrations as high as 12 $\mu$M. Thus, inhibition appears to be quite specific for DPM.

*DPM Inhibition Is Noncompetitive: A DPM-Specific Binding Site.* An initial-rate assessment of the mechanism of DPM inhibition required that the kinetic constants governing the forward reaction be determined (see Table 1 and Materials and Methods). The steady-state affinities of the E and E·ATP forms of the enzyme for mevalonate ($K_{i\,mev}$ and $K_{m\,mev}$, respectively) are 44 and 27 $\mu$M, respectively. $K_i$ and $K_m$ for ATP are considerably larger, 1.4 and 0.85 mM, respectively. The rate of turnover of the enzyme at saturating concentrations of both substrates is 228 $s^{-1}$. These constants are comparable to those associated with mevalonate kinases from other organisms (*15*−*17*).

DPM was tested as an inhibitor against mevalonate and ATP in a classical initial-rate inhibition study (see Table 2). Mutually exclusive binding of the substrate and inhibitor (competitive binding) predicts 1/*V* versus 1/[S] lines that intersect on the 1/*V* axis; $V_{max}$ is not influenced by the inhibitor at an infinite substrate concentration. If, on the other hand, the substrate and inhibitor can bind to the enzyme

Table 2: Steady-State and Equilibrium-Binding Affinity of DPM and *S. pneumoniae* MVK[a]

| steady-state constants ($\mu$M) | | | | equilibrium-binding constants ($\mu$M)[c] | |
|---|---|---|---|---|---|
| variable mevalonate | | variable $Mg^{2+}$ATP | | | |
| $K_{is}$[b] | $K_{ii}$[b] | $K_{is}$ | $K_{ii}$ | apo-MVK[d] | MVK·Mev·$Mg^{2+}$AMP-PNP[d] |
| $0.52 \pm 0.06$ | $0.70 \pm 0.04$ | $0.40 \pm 0.02$ | $0.84 \pm 0.03$ | $0.63 \pm 0.06$ | $0.53 \pm 0.02$ |

[a] Constants are presented with their standard error. [b] $K_{is}$ and $K_{ii}$ are the steady-state affinities of DPM for the E·$S_2$ and E·$S_1$·$S_2$ complexes, respectively, where $S_1$ and $S_2$ are the nonvariable and variable substrates, respectively (see panels A and B of Figure 3). [c] Determined using native protein fluorescence (see text). [d] Enzyme form for which DPM affinity was measured.

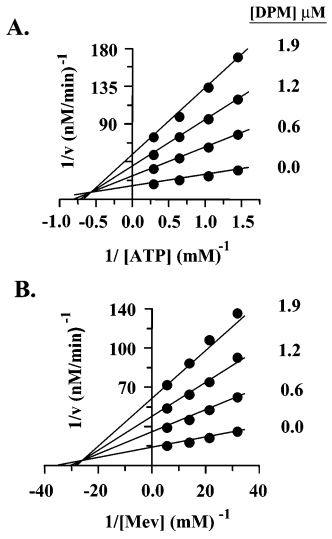


FIGURE 4: Diphosphomevalonate inhibition of *S. pneumoniae* MVK is noncompetitive vs ATP and mevalonate. (A) DPM inhibition vs ATP. The initial rate of the reaction is plotted in double-reciprocal format as a function of substrate (ATP) and inhibitor (DPM) concentrations. The assay conditions were as follows: MVK (40 nM), ATP (0.70, 1.0, 1.6, and 3.7 mM; 1.0−4.6$K_m$), DPM (at the indicated concentrations), mevalonate (190 $\mu$M, 7$K_m$), $MgCl_2$ ([nucleotide] + 1.0 mM), pyruvate kinase (10 units/mL), lactate dehydrogenase (20 units/mL), PEP (1.0 mM), NADH (0.30 mM), KCl (50 mM), 2-$\beta$ME (0.14%), and Hepes/$K^+$ (50 mM, pH 8.0) at 25 ± 2 °C. (B) DPM inhibition vs mevalonate. The experimental design and conditions were identical to those for panel A except that the mevalonate concentrations were varied (32, 48, 90, and 240 $\mu$M Mev; 1−9$K_m$) and the concentration of ATP was fixed at 5.0 mM (6$K_m$). The solid lines represent the behavior predicted by the best-fit parameters obtained by statistically fitting the data to a linear noncompetitive inhibition model using the *NONCOMP* algorithm (*14*).

simultaneously (noncompetitive binding), the substrate cannot drive the inhibitor from the enzyme, and a $V_{max}$ effect is observed. DPM inhibition is clearly noncompetitive against both ATP and mevalonate (Figure 4A, B); thus, each of these ligands has a distinct and nonoverlapping binding site, one of which is the DPM-specific regulatory site. Intersection of the 1/*V* versus 1/[S] lines above the 1/[S] axis indicates that the affinity of DPM for the enzyme decreases slightly (~1.5-fold) upon binding of the substrate.

*DPM Binding at Equilibrium.* To define further the interactions of DPM and mevalonate kinase, their equilibrium-binding affinity was measured using fluorescence spectroscopy. DPM binding causes the fluorescent intensity of mevalonate kinase to increase 1.5-fold ($\lambda_{ex}$ = 278 nm; $\lambda_{em}$ = 337 nm). The binding of DPM and apo-MVK is fit well using a simple, non-allosteric binding model, in which $K_d$ = 0.63 ± 0.06 $\mu$M (Figure 5A and Table 2). The stoichiometry of the DPM−enzyme interaction was determined in a titration experiment in which the enzyme active site concentration was set to 66$K_d$. Under this condition, only a small fraction of the DPM partitions into solution until the unliganded enzyme concentration approaches $K_d$, a region that occurs immediately prior to the plateau (where the ligand is in excess over the binding site). This short, transitional region defines the point at which the ligand concentration begins to exceed that of the active site, thereby yielding the binding stoichiometry, which, in this case, is one DPM bound per mevalonate kinase dimer (0.50 ± 0.01 DPM/active site) (Figure 5B). The native *S. pneumoniae* mevalonate kinase,

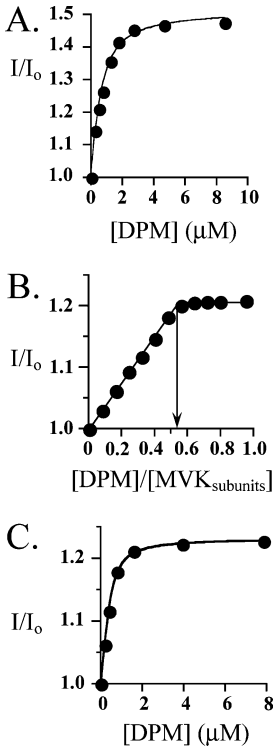


FIGURE 5: Equilibrium-binding interactions of DPM and mevalonate kinase. (A) Titration of apoMVK with DPM. The titration solution contained MVK (0.20 $\mu$M), KCl (50 mM), 2-ME (0.14 vol %), and Hepes/$K^+$ (50 mM, pH 8.0) at 25 ± 2 °C. The protein was excited at 278 nm, and the fluorescence was monitored at 337 nm. $K_d$ (0.63 $\mu$M) was obtained by statistically fitting the data to a single-site binding model, and was used to generate the solid line that passes through the data. (B) Binding stoichiometry. The stoichiometry was determined at a high (66$K_d$) active site concentration (see the text). The protein was excited at 278 nm, and emitted light was detected at 337 nm. The best-fit stoichiometry, 0.50 ± 0.01, was obtained by statistically fitting the data to a simple binding model in which the stoichiometry was varied, and in which $K_d$ was fixed at 0.63 $\mu$M (see the panel A study). The behavior predicted by the best-fit stoichiometry is described by the solid line that passes through the data. The titration solution contained MVK (25 $\mu$M, monomer), $MgCl_2$ (3.0 mM), KCl (50 mM), 2-$\beta$ME (0.14%), and Hepes/$K^+$ (50 mM, pH 8.0) at 25 ± 2 °C. (C) Binding of DPM to the E·ATP·mevalonate complex. The protein was excited at 297 nm (which was sufficiently long to avoid inner-filter effects of the nucleotide), and emitted light was detected at 333 nm; varying the AMP-PNP as low as 3.0 mM did not affect $K_d$ (data not shown). $K_d$ (0.53 $\mu$M) was obtained by statistically fitting the data to a nonallosteric binding model, and was used to generate the solid line that passes through the data. The solution contained MVK (0.20 $\mu$M), AMP-PNP (12 mM, 4.6$K_i$), $MgCl_2$ (14 mM), mevalonate (0.50 mM, 18$K_m$), KCl (50 mM), 2-ME (0.14%), and Hepes/$K^+$ (50 mM, pH 8.0) at 25 ± 2 °C. The data points shown in panels A−C represent the averages of at least four determinations. The model used to obtain the best-fit $K_d$ values used a binding stoichiometry of 0.50 DPM per MVK active site.

like the *Methanococcus jannaschii* and mammalian mevalonate kinases (*15*, *16*, *18*), is a dimer, and its apparent native molecular mass (68.0 ± 1.0 kDa; see Materials and Methods) is twice that of its subunit (~32 kDa). These finding indicate that one molecule of DPM binds per native enzyme molecule, and suggest that DPM may bind at a subunit interface.

To confirm the noncompetitive nature of the DPM inhibition indicated by the steady-state measurements, the affinity of DPM for the enzyme was determined in the presence of a saturating concentration of mevalonate and the nonreactive ATP analogue, AMP-PNP. These compounds,

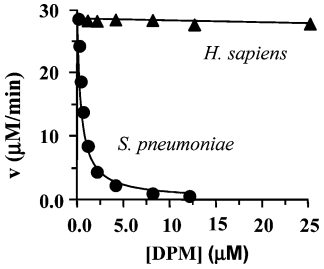


FIGURE 6: Human MVK is not inhibited by DPM. The initial rates of the forward reaction catalyzed by the human and *S. pneumoniae* enzymes are plotted as a function of DPM concentration. The assay conditions were as follows: human (37 nM) or *S. pneumoniae* (48 nM) mevalonate kinase, mevalonate (30 $\mu$M, $\sim 1K_m$ for either system), ATP ($\sim 1K_m$, 60 and 800 $\mu$M for the human and *S. pneumoniae* enzymes, respectively), $MgCl_2$ ([ATP] + 1 mM), KCl (50 mM), 2-ME (20 mM), and Hepes/$K^+$ (50 mM, pH 8.0) at 25 $\pm$ 2 °C.

which form a Michaelis-like complex (E·AMP-PNP·mevalonate), will appear to weaken the affinity of DPM as their concentrations increase if the substrate and DPM bind competitively; alternatively, the absence of an effect on the DPM binding affinity argues for a separate, DPM-specific binding site.

To ensure that AMP-PNP binding is well behaved, and to assess its affinity for the E·mevalonate complex, it was tested as a competitive inhibitor versus ATP in an initial-rate inhibition study. AMP-PNP binding is indeed competitive against ATP, and its affinity for the E·mevalonate complex ($K_i = 2.6$ mM) is approximately half that of ATP (data not shown). It should be noted that unlike DPM, mevalonate and/or AMP-PNP binding does not change the fluorescent behavior of the enzyme, which also argues for a unique DPM binding site. Titration of the E·AMP-PNP·mevalonate complex with DPM is shown in Figure 5C. The affinity of DPM for the E·AMP-PNP·mevalonate complex ($K_d = 0.53 \pm 0.02$ $\mu$M; see Table 2) is experimentally indistinguishable from its affinity for the apoenzyme ($K_d = 0.63 \pm 0.06$ $\mu$M). The conditions of this experiment are such that if DPM binding were competitive against mevalonate and/or AMP-PNP, its apparent affinity would have decreased significantly [5.6−67-fold depending on which ligand(s) binds competitively]. These results add additional, strong support for a DPM-specific binding site.

*Human MVK Is Not Inhibited by DPM.* To begin to assess the efficacy of the DPM binding site as an antimicrobial target, it was important to know whether the DPM inhibition observed with the *S. pneumoniae* enzyme also occurs with the human enzyme. The mammalian and streptococcal mevalonate kinases are both members of the GHMP kinase family, yet their primary sequences are quite diverse. The two sequence classes exhibit a modest level of identity of $\sim$20%, and the mammalian sequences contain an additional $\sim$100 residues that are found in clusters throughout their primary sequences. These differences suggested that mammalian enzymes might not harbor the allosteric site.

To determine the extent to which the human mevalonate kinase is inhibited by DPM, the enzyme was cloned, expressed in *E. coli*, and purified to $\geq$95% homogeneity (see Materials and Methods), and the effects of DPM on the initial rate of the forward reaction were tested. In preparation for the inhibition study, the kinetic constants for the forward reaction were determined (Table 1; see Materials and Methods). The constants ($K_{m\ ATP} = 57$ $\mu$M, $K_{m\ mevalonate} = 33$ $\mu$M, and $k_{cat} = 20$ $s^{-1}$) agree well with a previous characterization of the human MVK (*16*). The effects of DPM on the initial rate of the forward reaction catalyzed by the human and *S. pneumoniae* mevalonate kinases are compared in Figure 6. The streptococcal enzyme is sensitive to DPM in the sub-micromolar range, while the human enzyme exhibits no significant inhibition at DPM concentrations as high as 25 $\mu$M.

## CONCLUSIONS

Isoprenoid biosynthesis in the pneumococcus can be allosterically inhibited by the binding of DPM to mevalonate kinase. Binding is noncompetitive against the enzyme's substrates, and therefore, inhibition cannot be slowed by an inhibitor-induced accumulation of substrates, which could occur *in vivo*. The lack of DPM inhibition of the human mevalonate kinase provides the opportunity to selectively inhibit the organism in a human host. Mevalonate passes from media into streptococcus (*4*), suggesting that mevalonate analogues, like the 6-fluoro derivatives (*19*), will also be taken up and perhaps phosphorylated *in situ* to produce an inhibitor, a pro-drug strategy. Inhibitors that resemble DPM will likely also inhibit DPM decarboxylase. Dual-target inhibition is particularly powerful because the net potency of an inhibitor can be as high as the product of its potency at each site of inhibition.

Without a functioning mevalonate pathway, pathogenic *S. pneumoniae* is unable to survive in mouse lung, virulence is severely attenuated, and the concentration of mevalonate in human serum (20−80 nM) is too low to complement strains with an inactive pathway (*4*, *20*). This organism appears to have a molecular Achilles heel, the DPM-binding site, and it should be possible to use DPM as a template to develop antibiotics for inhibiting isoprenoid biosynthesis in *S. pneumoniae* and, hopefully, cure pneumococcal disease.

## NOTE ADDED AFTER ASAP PUBLICATION

This paper was published prematurely 12/04/04. Figure 4 has been replaced, and the value in the second to last line of text in the column below Figure 4 has been changed. The citation for ref *12* has also been completed. The correct version of this paper was published 12/06/04.

## REFERENCES

1. Kharel, Y., and Koyama, T. (2003) Molecular analysis of cis-prenyl chain elongating enzymes, *Nat. Prod. Rep. 20*, 111−118.
2. Wang, K. C., and Ohnuma, S. (2000) Isoprenyl diphosphate synthases, *Biochim. Biophys. Acta 1529*, 33−48.
3. Fujihashi, M., Zhang, Y. W., Higuchi, Y., Li, X. Y., Koyama, T., and Miki, K. (2001) Crystal structure of cis-prenyl chain elongating enzyme, undecaprenyl diphosphate synthase, *Proc. Natl. Acad. Sci. U.S.A. 98*, 4337−4342.
4. Wilding, E. I., Brown, J. R., Bryant, A. P., Chalker, A. F., Holmes, D. J., Ingraham, K. A., Iordanescu, S., So, C. Y., Rosenberg, M., and Gwynn, M. N. (2000) Identification, evolution, and essentiality of the mevalonate pathway for isopentenyl diphosphate biosynthesis in Gram-positive cocci, *J. Bacteriol. 182*, 4319−4327.
5. Schrag, S. J., McGee, L., Whitney, C. G., Beall, B., Craig, A. S., Choate, M. E., Jorgensen, J. H., Facklam, R. R., and Klugman, K. P. (2004) Emergence of *Streptococcus pneumoniae* with very-high-level resistance to penicillin, *Antimicrob. Agents Chemother. 48*, 3016−3023.

6. McGee, L., McDougal, L., Zhou, J., Spratt, B. G., Tenover, F. C., George, R., Hakenbeck, R., Hryniewicz, W., Lefevre, J. C., Tomasz, A., and Klugman, K. P. (2001) Nomenclature of major antimicrobial-resistant clones of *Streptococcus pneumoniae* defined by the pneumococcal molecular epidemiology network, *J. Clin. Microbiol. 39*, 2565−2571.
7. Hawley, L. A., Walker, F., and Whitney, C. G. (2002) in *VPD Surveillance Manual*, pp 1−14, Centers for Disease Control and Prevention, Atlanta.
8. Henriques Normark, B., Novak, R., Ortqvist, A., Kallenius, G., Tuomanen, E., and Normark, S. (2001) Clinical isolates of *Streptococcus pneumoniae* that exhibit tolerance of vancomycin, *Clin. Infect. Dis. 32*, 552−558.
9. McCullers, J. A., English, B. K., and Novak, R. (2000) Isolation and characterization of vancomycin-tolerant *Streptococcus pneumoniae* from the cerebrospinal fluid of a patient who developed recrudescent meningitis, *J. Infect. Dis. 181*, 369−373.
10. Mitchell, L., and Tuomanen, E. (2001) Vancomycin-tolerant *Streptococcus pneumoniae* and its clinical significance, *Pediatr. Infect. Dis. J. 20*, 531−533.
11. Shinefield, H. R., and Black, S. (2000) Efficacy of pneumococcal conjugate vaccines in large scale field trials, *Pediatr. Infect. Dis. J. 19*, 394−397.
12. Andreassi, J. L., II, and Leyh, T. S. (2004) Molecular functions of conserved aspects of the GHMP kinase Family, *Biochemistry 43*, 14594−14601.
13. Pilloff, D., Dabovic, K., Romanowski, M. J., Bonanno, J. B., Doherty, M., Burley, S. K., and Leyh, T. S. (2003) The kinetic mechanism of phosphomevalonate kinase, *J. Biol. Chem. 278*, 4510−4515.
14. Cleland, W. W. (1979) Statistical analysis of enzyme kinetic data, *Methods Enzymol. 63*, 103−138.
15. Chu, X., and Li, D. (2003) Cloning, expression, and purification of His-tagged rat mevalonate kinase, *Protein Expression Purif. 27*, 165−170.
16. Potter, D., and Miziorko, H. M. (1997) Identification of catalytic residues in human mevalonate kinase, *J. Biol. Chem. 272*, 25449−25454.
17. Voynova, N. E., Rios, S. E., and Miziorko, H. M. (2004) *Staphylococcus aureus* mevalonate kinase: Isolation and characterization of an enzyme of the isoprenoid biosynthetic pathway, *J. Bacteriol. 186*, 61−67.
18. Huang, K. X., Scott, A. I., and Bennett, G. N. (1999) Overexpression, purification, and characterization of the thermostable mevalonate kinase from *Methanococcus jannaschii*, *Protein Expression Purif. 17*, 33−40.
19. Reardon, J. E., and Abeles, R. H. (1987) Inhibition of cholesterol biosynthesis by fluorinated mevalonate analogues, *Biochemistry 26*, 4717−4722.
20. Popjak, G., Boehm, G., Parker, T. S., Edmond, J., Edwards, P. A., and Fogelman, A. M. (1979) Determination of mevalonate in blood plasma in man and rat. Mevalonate "tolerance" tests in man, *J. Lipid Res. 20*, 716−728.

BI048075T